Measurement and Comparison of Wi-Fi and Super Wi-Fi Indoor Propagation Characteristics in a Multi-Floored Building

Gyumin Hwang, Kyubo Shin, Sanghyeok Park, and Hyoil Kim

Abstract: **Super Wi-Fi is a Wi-Fi-like service exploiting TV white space (WS) which is expected to achieve larger coverage than today's Wi-Fi thanks to its superior propagation characteristics. Super Wi-Fi has been materialized as an international standard, IEEE 802.11af, targeting indoor and outdoor applications, and is undergoing worldwide field tests. This paper demonstrates the true potential of indoor Super Wi-Fi, by experimentally comparing the signal propagation characteristics of Super Wi-Fi and Wi-Fi in the same indoor environment. Specifically, we measured the wall and floor attenuation factors and the path-loss distribution at 770 MHz, 2.401 GHz, and 5.540 GHz, and predicted the downlink capacity of Wi-Fi and Super Wi-Fi. The experimental results have revealed that TVWS signals can penetrate up to two floors above and below, whereas Wi-Fi signals experience significant path loss even through a single floor. It has been also shown that Super Wi-Fi mitigates shaded regions of Wi-Fi by providing almost-homogeneous data rates within its coverage, performs comparable to Wi-Fi utilizing less bandwidth, and always achieves better spectral efficiency than Wi-Fi. The observed phenomena imply that Super Wi-Fi is suitable for indoor applications and has the potential of extending horizontal and vertical coverage of today's Wi-Fi.**

Index Terms: **ISM, Super Wi-Fi, Wi-Fi, TV white space, UNII**

I. INTRODUCTION

COGNITIVE Radio (CR) enables opportunistic access to spectrum white space (WS) via software-reconfigurable agile radio devices such as software defined radios (SDRs). A spectrum WS refers to a frequency-time resource block in the legacy spectrum bands temporarily left unused by their licensed users. In particular, WS in the TV bands, called TVWS, has been opened up in the US by the FCC [1] for opportunistic unlicensed use, and is expected to be made available in other countries as well. TVWS is designated to a specific portion of VHF/UHF bands, such as 54–698 MHz in the US [1] and 470–790 MHz in Europe [2], [3].

Manuscript received January 12, 2015; approved for publication by Dusit (Tao) Niyato, Division III Editor, September 7, 2015.

G. Hwang is with Sysmate, Inc., Daejeon, 35233, Korea, e-mail: hkm73560@sysmate.com.

K. Shin, S.Park, and H. Kim are with the School of Electrical and Computer Engineering, Ulsan National Institute of Science and Technology (UNIST), Ulsan, 44919, Korea, e-mail: {kyubo, parksh31, hkim}@unist.ac.kr.

Hyoil Kim is the corresponding author.

The work described in this paper was supported in part by Basic Science Research Program through the National Research Foundation of Korea (NRF) funded by the Ministry of Education (NRF-2014R1A1A2056438), and by IITP grant funded by the Korea government (MSIP) (No. B0126-15-1064, Research on Near-Zero Latency Network for 5G Immersive Service).

Digital object identifier 10.1109/JCN.2016.000062

Super Wi-Fi is a commercial CR application for personal/portable devices, designed to provide Wi-Fi like service by utilizing TVWS. Thanks to the superior characteristics of TVWS compared to ISM/UNII bands, such as smaller path loss, stronger wall-penetration, and stronger diffractiveness, Super Wi-Fi is expected to achieve larger coverage than today's Wi-Fi [4]. Super Wi-Fi has also been materialized as an international standard, IEEE 802.11af [5], and will soon be deployed in the consumer market.

Super Wi-Fi is considered suitable for both indoor and outdoor uses. Outdoor Super Wi-Fi is ideal for deploying large-scale wireless backbone that provides connection to the Internet to the last-mile small-scale wireless networks like Wi-Fi. Moreover, it is also considered for cellular traffic offloading due to its large coverage. Indoor Super Wi-Fi can achieve room-to-room coverage with fairly well distributed data rates thanks to its strong diffraction and wall-penetration ability. Therefore, one of the Super Wi-Fi's target applications is video streaming within the home area.

In this paper, we demonstrate the benefit of deploying Super Wi-Fi indoors by identifying its superior properties to Wi-Fi via experimental studies. Although there exist various work modeling the indoor signal propagation either at VHF/UHF bands [6]–[10] or at ISM/UNII bands [11]–[13], none of them has provided measurement-based comparison of the propagation characteristics of the two bands in the same indoor environment. Hence, we performed extensive experiments for both Wi-Fi and Super Wi-Fi in the same building structure and compared their characteristics, with an objective of identifying the potential of Super Wi-Fi in mitigating the limitations of indoor Wi-Fi such as small coverage, shaded regions, performance anomaly, etc.

The contribution of this paper is three-fold. First, we performed extensive measurements to compare the signal propagation characteristics of Wi-Fi and Super Wi-Fi in the same indoor environment, in terms of wall and floor attenuation factors, path loss, and path loss exponents, while applying the measured data to the widely-accepted path loss models. Second, we demonstrate the efficacy of exploiting TVWS for future indoor Super Wi-Fi applications with more favorable characteristics such as extended coverage and almost-homogeneous data rate distribution. Lastly, we estimate the average downlink capacity of an indoor Super Wi-Fi network and compare it with that of Wi-Fi.

The rest of the paper is organized as follows. Section II reviews related work, and then Section III presents the experimental setup. Section IV demonstrates the measurement results including wall and floor attenuation factors and the path loss of TVWS, ISM, and UNII bands. Section V estimates and com-

pares the average downlink capacity of Wi-Fi and Super Wi-Fi, and the paper concludes with Section VI.

II. RELATED WORK

There have been various studies on indoor signal propagation characteristics via analytical modeling and field measurements, focusing on either VHF/UHF or ISM/UNII bands.

Regarding the VHF/UHF bands, [6] and [7] measured the indoor path loss in buildings at 914 MHz and at 917 MHz, respectively, considering floor and wall attenuations. In [8], the waveguide effect in indoor hallways at 850–950 MHz was studied via measurements. In [9], the features of office buildings that influence signal propagation at 900 MHz were investigated based only on theoretical models and computer simulations. More recently, [14] measured outdoor temporal and spatial characteristics of DTV signals at 713 MHz, and [10] performed indoor measurements at 625 MHz and compared the results with the ray-tracing predictions.

Regarding the ISM/UNII bands, [11] measured in-building path loss and wall attenuation at 2.5 GHz, while [12] measured indoor path loss at 5.2 GHz with wall and floor attenuation. On the other hand, [13] presented link throughput based signal propagation characterization, instead of utilizing the path loss, in an office building at 2.4 GHz.

Nevertheless, none of the aforementioned work compared the characteristics of TVWS and Wi-Fi bands in the same indoor environment. Although [15] and [4] have compared the signal propagation of TVWS and ISM, those attempts were merely based on an analytical prediction, without any actual measurements. Since it is usually hard to accurately model indoor signal propagation due to various obstacles and structural dependencies, a field measurement based approach is crucial in predicting the efficacy of TVWS in indoor environments that have been traditionally served by Wi-Fi.

III. EXPERIMENTAL SETUP

This section describes the experimental setup including measurement instruments, signal formats, measured spectrum, and tested indoor environments.

A. Measurement Instruments

Measurements were performed by a popular SDR device, USRP™ by Ettus Research [16]. The USRP consists of a mother board and a replaceable daughter board, where the former processes data through FPGA and ADC/DAC and the latter operates as a tunable transceiver. USRP is agile enough to support frequency bands from DC to 6 GHz, covering both TVWS and ISM/UNII bands, and can support any user-implemented modulation schemes and frame formats thus eliminating unwanted side effects from the factors not directly related to the signal characteristics.

In our measurements, we used USRP N210 combined with one of three daughter boards, XCVR 2450, WBX, and SBX, selectively chosen according to the spectrum band to measure. A USRP system is connected to an external host computer via the Gigabit Ethernet through which baseband data are streamed

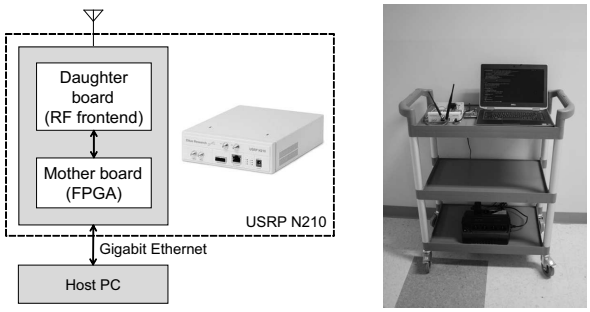

Fig. 1. Block diagram of USRP and mobile experimental setup: (a) Block diagram and (b) experimental setup.

to/from the host. The host controls the USRP via the USRP hardware driver (UHD), which can be installed separately or with third-party applications like GNU Radio [17] and LabVIEW. We used a host PC configured with Intel Core i7-2620M (2.7 GHz, 2 cores), 8 GB RAM, 180 GB SSD, Ubuntu 11.10, GNU Radio version 3.4.2, and UHD 003.003.000. Fig. 1 shows the block diagram of a USRP N210 system and the experimental setup of a mobile USRP.

Note that USRP's transmit power is controlled by two configurable parameters, *gain* and *amp*, where the former represents the analog gain at the USRP's power amplifier, and the latter represents the digital amplitude of the signal samples. By jointly controlling the two parameters, the USRP can transmit a signal as strong as 100 mW, which coincides with the usual transmit power of commercial Wi-Fi access points (APs) and the maximum allowed equivalent isotropically radiated power (EIRP) of portable white space devices (WSDs) regulated by FCC [1]. Therefore, in our experiments we have carefully set the gain and amp parameters such that the transmit power of the USRP can be maximized within the 100 mW power budget.[1]

B. Signal Modulation

In each experiment, a pair of USRP transceivers transmits and receives OFDM signals with 16 subcarriers that are generated by RawOFDM [18], an open-source OFDM implementation for GNU Radio. The USRP receiver built upon RawOFDM demodulates the OFDM signal and measures the received SNR. We have chosen OFDM for the measurement since modern Wi-Fi and Super Wi-Fi standards are based on OFDM, as in IEEE 802.11ac and IEEE 802.11af. Therefore, using OFDM signals makes it possible to predict their signal characteristics in practical scenarios more accurately.

The path loss between the pair of transceivers can be obtained from the measured received signal-to-noise ration (SNR) as follows. First, the two USRPs are directly connected via a 50 Ω SMA-SMA cable concatenated with a 50 dB attenuator, and the receiver measures the SNR of the transmitted signal. Then, the measured SNR is added by 50 dB to account for the reduced

[1]Maximizing the power does not necessarily imply maximizing the gain and amp parameters due to the design of USRP. When the two parameters are increased beyond certain thresholds, the transmit power tends to saturate or sometimes even decrease. Hence, we have manually tuned the parameters in each of the following experiments.

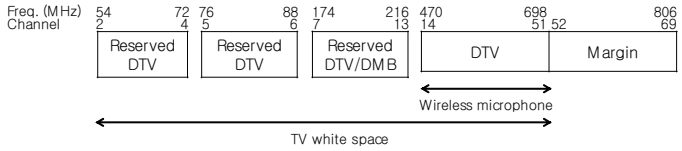

Fig. 2. TVWS in Korea.

Table 1. Experimental radio frequencies close to TVWS in Korea (with bandwidth larger than 10 kHz).

Frequency (MHz)	48.5	116.3	150.06	155.3
Bandwidth (kHz)	16	25	16	16
Frequency (MHz)	219.5	451.2	456.2	770
Bandwidth (kHz)	16	16	15	200

signal strength by the attenuator, and the resulting SNR can be thought of as a 'transmitted SNR'. Finally, the transmitted SNR is compared to the received SNR measured over the air (with transmitting and receiving antennas), where the difference between them becomes the path loss.

C. Spectrum Bands

In Korea, TVWS lies in 54–698 MHz (TV channels 2–51) as shown in Fig. 2. Since the TVWS in Korea is not yet open for unlicensed use, we have conducted our measurements at 770 MHz with the bandwidth of 200 kHz which is allowed for experimental radio stations according to the Korean Radio Regulation Law. 770 MHz has been chosen because it provides the largest bandwidth among the experimental frequency bands close to the TVWS, as shown in Table 1.

For Wi-Fi, we performed experiments at 2.401 GHz in the ISM bands and at 5.540 GHz in the UNII bands. For a fair comparison between TVWS and ISM/UNII, the channel bandwidth was also set as 200 kHz.

Note that the chosen bands helped suppress unwanted but unexpected interferences in signal measurements because (1) at 770 MHz, our devices were the only registered and operating experimental radios at UNIST, (2) at 2.401 GHz and 5.540 GHz, each with 200 kHz bandwidth, there were free of interfering Wi-Fi stations since the chosen band at 2.401 GHz does not overlap with channel 1 in [2.402, 2.422] GHz and the chosen band at 5.540 GHz had no operational Wi-Fi stations in the building. Fig. 3 presents our monitoring results at the chosen three bands that confirm the absence of interferers. Note that the measured SNR with 200 kHz bandwidth will be scaled to larger bandwidths in subsection V-A.

D. Indoor Environment

All measurements were conducted on the third, fourth and fifth floors of the EB2 building at UNIST. The building was constructed with steel reinforced concrete, marble floors, metal doors, and concrete and ply wood walls. In addition, the building structure includes two staircases, two passenger and one cargo elevators, and several utility rooms in the central area. Fig. 4 illustrates the floor plan.

In the described indoor environment, the minimum separation between the transmitter-receiver pair was set as 2 meters to place them in a far-field region [19], which is beyond the distance d_f

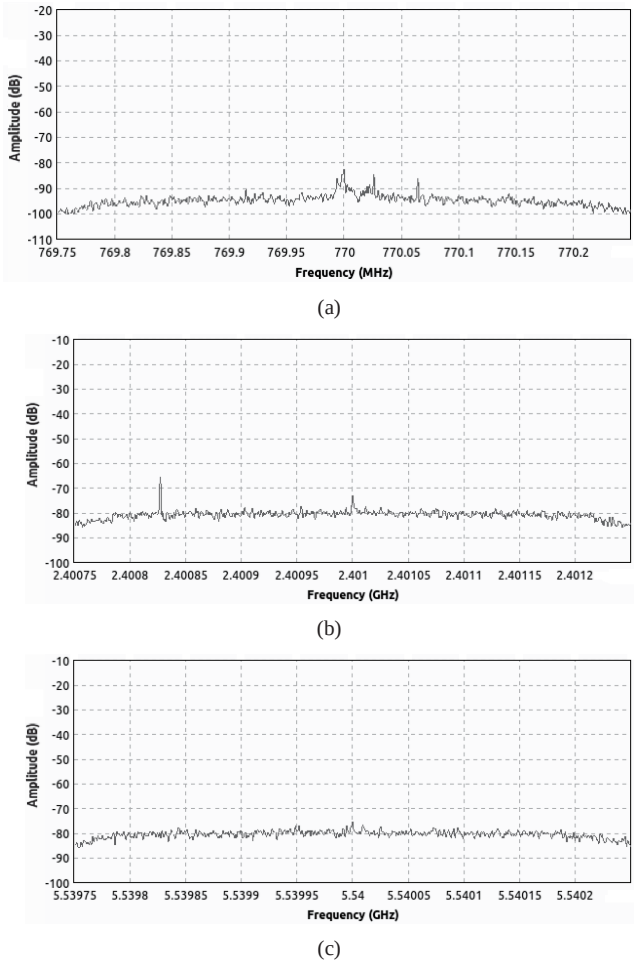

Fig. 3. Spectrum monitoring measurements at three chosen bands: (a) 770 MHz, (b) 2.401 GHz, and (c) 5.540 GHz.

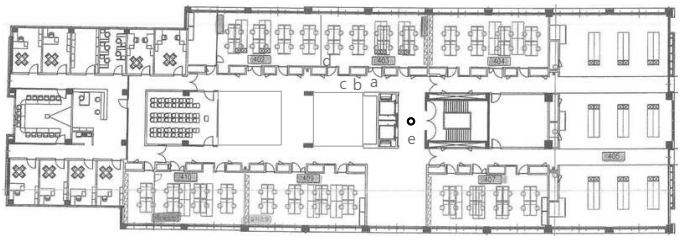

Fig. 4. The floor plan of the EB2 building at UNIST.

such that

$$d_f = \max\left\{2D^2/\lambda, 5D, 1.6\lambda\right\} \quad (1)$$

where λ is the wavelength and D is the largest dimension of an antenna. In our experiments, the 770 MHz antenna was 14.6 cm long resulting in $d_f = 73$ cm and the 2.401 & 5.540 GHz antenna was 15 cm long leading to $d_f = 75$ cm for 2.401 GHz and $d_f = 83.1$ cm for 5.540 GHz, respectively.

IV. COMPARISON OF SPECTRUM CHARACTERISTICS BETWEEN TVWS AND ISM

Super Wi-Fi has better wall-penetrability and experiences less path loss than Wi-Fi thanks to its sub-GHz spectrum, which is beneficial for indoor environments with various obstacles like

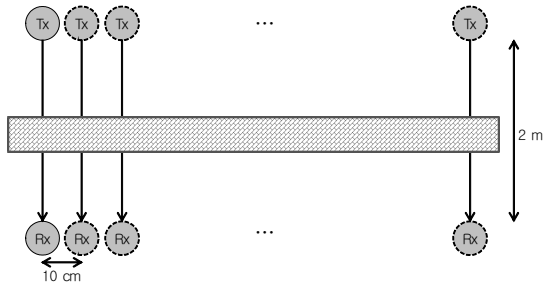

Fig. 5. WAF measurement procedure.

Table 2. WAF and its standard deviation σ at 770 MHz and 2.401 GHz.

	f_c (GHz)	WAF (dB)	WAF (dB/cm)	σ (dB)
Thin ply wood wall	0.770	2.424	0.134	2.307
	2.401	8.974	0.498	4.888
Thick ply wood wall	0.770	3.131	0.025	2.597
	2.401	17.72	0.144	5.716
Metal door	0.770	2.683	0.536	1.907
	2.401	13.31	2.664	4.714
Compound wall	0.770	2.673	0.356	0.998
	2.401	18.59	2.479	4.101

Table 3. WAF of the metal door (in dB/cm).

	770 MHz	2.401 GHz
At 1.3 meters	0.553	2.121
At 0.9 meters	0.519	2.995

walls, doors, and floors. In this section, we demonstrate the indoor characteristics of Super Wi-Fi and compare it with that of Wi-Fi through three metrics, wall attenuation factor (WAF), floor attenuation factor (FAF), and path loss. All measurements were taken in the EB2 building at UNIST, where the WAF and path loss experiments were conducted on the fourth floor and the FAF experiment was conducted throughout the third, fourth, and fifth floors.

A. Wall Attenuation Factor (WAF) Measurements

Fig. 4 presents four types of walls and doors, whose locations are marked as (a) metal door (5 cm thick), (b) thick ply wood wall (123 cm thick), (c) thin ply wood wall (18 cm thick), and (d) compound wall (7.5 cm thick, 97% urethane and 3% metal). WAF is defined as the path loss incurred by a wall (or a door), obtained by measuring the difference between the received SNRs *with* and *without* the wall. In each measurement, the tested wall was placed at the middle of a transceiver pair apart by 2 meters, and the transceivers were moved together along the wall in the step of 10 cm to measure 11–21 positions. The path loss was measured 5 times at each position, and all measurements were averaged to obtain the estimated WAF, to account for not perfectly homogeneous wall materials. Fig. IV-A depicts the procedure of WAF measurements.

The transmitting and receiving antennas were 1.3 meters above the floor when testing the ply wood and compound walls. In the case of the metal door, the measurements have been conducted at two different heights of 0.9 and 1.3 meters to examine the impact of the small window on the metal door (located at its mid-height) on the signal penetration. WBX and XCVR2450 daughter boards were used for the measurements performed at 770 MHz and 2.401 GHz, respectively.

Table 4. FAF (in dB) at 770 MHz and 2.401 GHz.

	770 MHz	2.401 GHz
Through 1 floor	0.701	14.368
Through 2 floors	7.980	N/A

Table 2 summarizes the WAF measurement results, where WAF is measured in both dB and dB/cm and f_c denotes the carrier frequency. In terms of the total attenuation in dB, the largest attenuation occurs with the thick ply wood wall at 770 MHz and with the compound wall at 2.401 GHz, implying that 2.401 GHz is more sensitive to the plated metal on the compound wall. The metal door, however, presents much less attenuation than the thick ply wood wall and the compound wall, because of the clear signal path through its windows. Overall, 770 MHz presents 4.5–39 times (in scalar) smaller attenuation than 2.401 GHz, e.g., 4.5 times for the thin ply wood wall and 39 times for the compound wall.

In terms of the normalized attenuation in dB/cm, the largest attenuation occurs with the metal door and the compound wall at both frequencies, showing that metal plating generally degrades signal penetration. In addition, the thin ply wood wall experiences larger attenuation per unit depth than the thick ply wood wall, indicating that non ply wood materials such as paint have a meaningful contribution to the wall attenuation.

Table 3 shows the impact of the position of window at the metal door. At 2.401 GHz, the door is better penetrated at the window height (i.e., 1.3 meters) than at 0.9 meters with the difference of 0.874 dB/cm, while 770 MHz presents a similar level of penetration between the two heights. This phenomenon seems to stem from the fact that signals are less diffractive at 2.401 GHz than at 770 MHz.

B. Floor Attenuation Factor (FAF) Measurements

In the FAF measurements, the transmitter was placed at a fixed location on the fifth floor while the receiver was moved along the corridor of the third, fourth, and fifth floor at the step of 30 cm and up to the distance of 17 meters, as shown in Fig. 6. The measurement area was selected to avoid the impact of staircases through which signals may travel between floors. Then, the FAF was estimated by measuring the difference between the average SNR on the fifth floor and the average SNR on the other floor (i.e., the third or the fourth).

Table 4 presents the measured FAF which is much smaller at 770 MHz than at 2.401 GHz. Notably, signal propagation at 770 MHz penetrated a single floor with a negligible signal loss of 0.701 dB and two floors with only 7.98 dB loss, which indicates that a single Super Wi-Fi AP may be able to serve up to 5 floors (i.e., 2 floors above and below). On the contrary, signal propagation at 2.401 GHz penetrated a single floor with 14.368 dB loss, which is more than 4 times larger (in scalar) than the FAF at 770 MHz over the two floors, and could not penetrate two

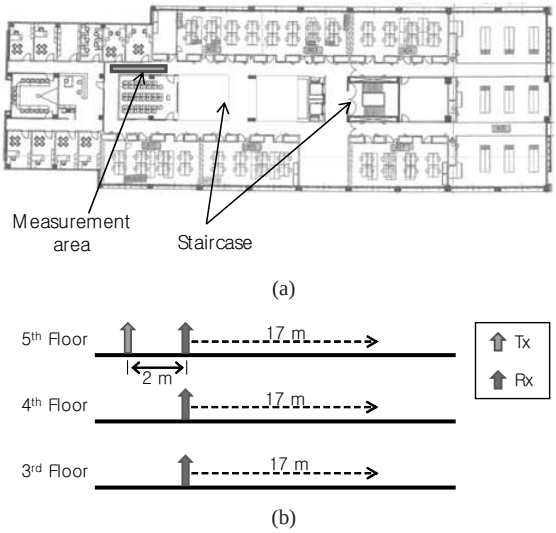

Fig. 6. FAF measurement scenario: (a) Measurement locations and (b) placement of transmitter and receiver.

Table 5. Average SNR (in dB) at 770 MHz, 2.401 GHz, and 5.540 GHz.

	770 MHz	2.401 GHz	5.540 GHz
rooms	26.93	20.78	5.20
corridors	27.99	20.74	16.69
overall	27.55	20.76	14.78

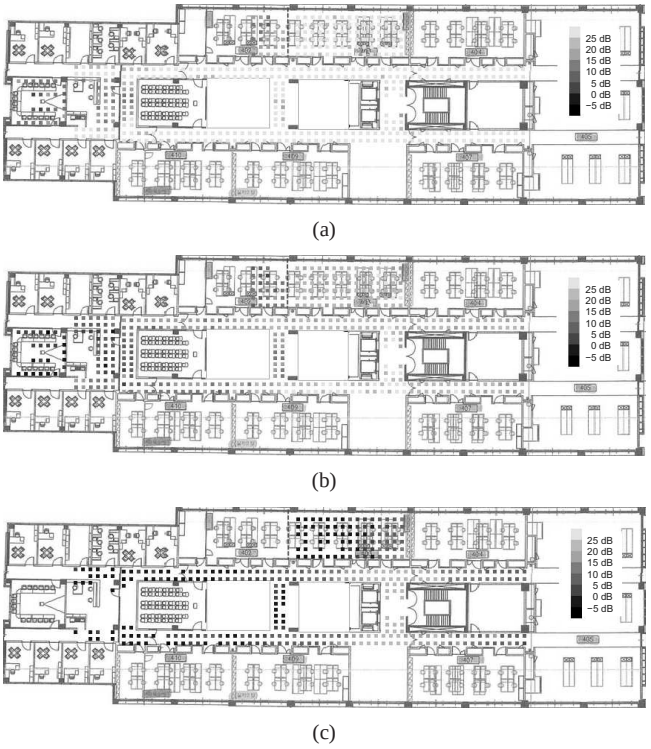

Fig. 7. SNR measurements at 770 MHz, 2.401 GHz, and 5.540 GHz: (a) 770 MHz, (b) 2.401 GHz, and (c) 5.540 GHz.

floors since the receiver experienced no decodable signals due to severe path-loss.

C. Path Loss Measurements

In the path loss measurement, the transmitter was placed at (e) in Fig. 4, and the receiver was moving around the floor at the step of 1 meter covering most of the corridors, two laboratory rooms, and a meeting room. Thanks to the symmetric building structure, the chosen locations well capture the signal propagation at uncovered areas. At each receiver location, SNR was measured 5 times by slightly varying the position by 10 cm. Three different frequencies, 770 MHz, 2.401 GHz, and 5.540 GHz, are measured with the same channel bandwidth of 200 kHz for fair comparison.

Fig. 7 illustrates the location-specific SNR measurements at the three bands.[2] As shown, Super Wi-Fi presents much enhanced SNR than the two types of Wi-Fi (at 2.401 and 5.540 GHz) in most locations, confirming its superior propagation characteristics. Table 5 summarizes the average SNR inside the rooms, in the corridors, and of the rooms/corridors combined, where 770 MHz presents 6.15–7.25 dB larger SNR than 2.401 GHz and 11.3–21.73 dB larger SNR than 5.540 GHz.

Using the measured SNRs, we have estimated the path loss exponent according to the simplified path loss model:

$$PL(d)[\text{dB}] = PL(d_0)[\text{dB}] + 10 \cdot \hat{n} \cdot \log_{10}(d/d_0), \quad (2)$$

where d (in meters) is the distance between the transceivers, d_0 is the reference distance, $PL(d)$ is the path loss at distance d, and $\hat{n}$ is the estimated path loss exponent. In this model, the impact of walls and obstacles is implicitly modeled by the path loss exponent. We have used $d_0 = 5.33$ meters.

Fig. 8 presents the measured path loss $PL(d)$ at varying distances for the three frequencies, where the red solid and the blue dotted lines represent the estimated path loss exponents at corridors and in rooms, respectively. Fig. 8(a) shows that the path loss stays low up to a certain distance and sharply increases beyond such a distance, thanks to the strong diffraction and small WAF at 770 MHz. Fig. 8(b), however, shows a steady increase in path loss with the distance, due to the weak diffraction and large WAF at 2.401 GHz. Such tendency is also seen from Fig. 8(c) regarding 5.540 GHz.

Table 6 presents the estimated path loss exponents $\hat{n}$. At 770 MHz, $\hat{n}$ is always smaller (thus better) than at 2.401 & 5.540 GHz, confirming its superior propagation characteristics. At any frequency, $\hat{n}$ is measured smaller in the corridors than that in the rooms because corridors introduce the waveguide effect while signals measured in the rooms experience additional attenuation at the walls enclosing the rooms.

D. Superior Characteristics of TVWS to ISM

The superior characteristics of TVWS to ISM/UNII, confirmed by the measurements, are summarized as follows.

- TVWS incurs 1.568–2.476 dB/cm less wall attenuation and 6.15–21.73 dB less path loss than ISM/UNII, and
- TVWS can penetrate up to two floors while ISM can't.

[2]A few uncolored locations at 5.540 GHz are due to no signals captured caused by severe path loss.

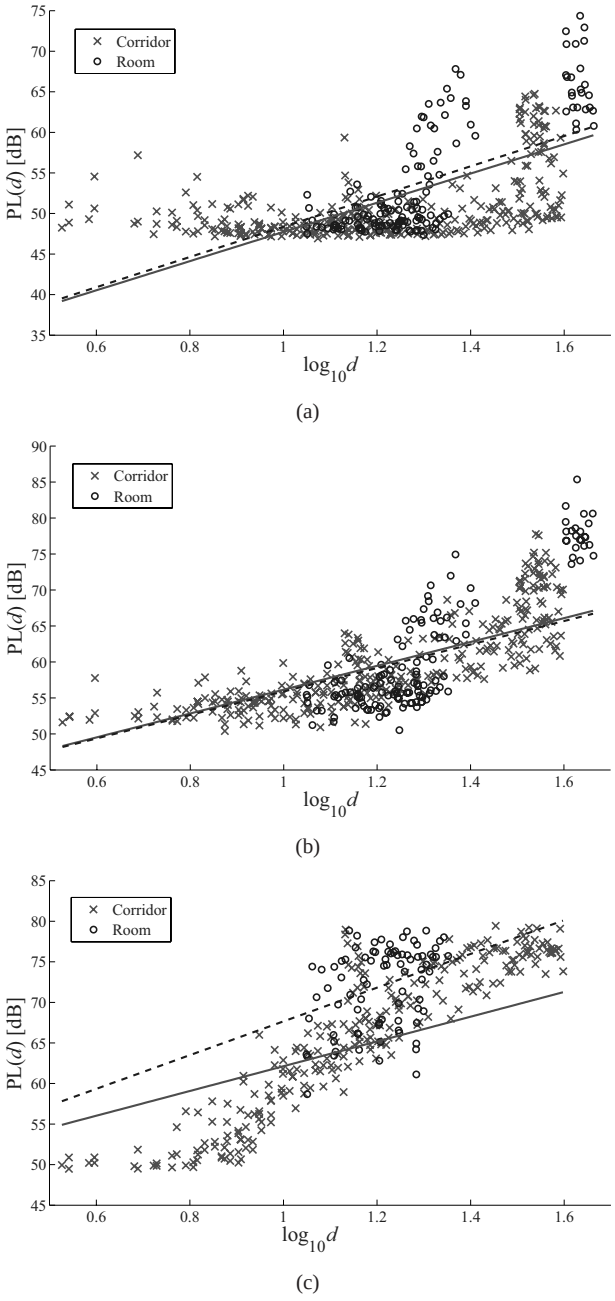

Fig. 8. Path loss measurement ($PL(d)$) vs. distance ($\log_{10} d$): (a) 770 MHz, (b) 2.401 GHz, and (c) 5.540 GHz.

Table 6. Estimated path loss exponents $\hat{n}$ and its standard deviation σ.

	f_c (GHz)	$\hat{n}$	σ
Rooms	0.770	0.80	0.94
	2.401	1.10	1.06
	5.540	4.62	1.10
Corridors	0.770	0.55	4.82
	2.401	0.99	6.58
	5.540	3.30	1.72
Overall	0.770	0.62	3.62
	2.401	0.98	4.93
	5.540	3.81	1.64

Table 7. Bandwidth-specific fade margin.

W_b (MHz)	0.2	6	12	20	24	40
F_σ (dB)	7.0	4.3	3.8	3.4	3.2	2.8

V. DOWNLINK CAPACITY ESTIMATION

In this section, we estimate the downlink capacity of Wi-Fi and Super Wi-Fi using the SNR measurements in Section IV. The channel bandwidth is 20 MHz in the Wi-Fi standards, e.g., IEEE 802.11a/n/ac, and 6, 7, or 8 MHz in the Super Wi-Fi standard, e.g., IEEE 802.11af [5], depending on the regions. We choose 6 MHz for Super Wi-Fi as regulated in Korea and the US. Since adjacent channels can be bonded together in both Wi-Fi and Super Wi-Fi, we consider 20, 40 MHz for Wi-Fi and 6, 12, 24 MHz for Super Wi-Fi.

A. Bandwidth-specific SNR Translation at USRP

For capacity estimation, it is necessary to properly scale the measurement taken with 200 kHz bandwidth in Section IV into the bandwidth of interest, i.e., 6, 12, 24 MHz for Super Wi-Fi and 20, 40 MHz for Wi-Fi. To do so, we hereby consider the bandwidth-dependent impact of small-scale fading to derive the bandwidth-specific fade margin. In [20], the fade margin F_σ (in dB) has been derived as a function of channel bandwidth W_b (in MHz) such as

$$F_\sigma(W_b)[\text{dB}] = k_1 - k_2 \log_{10} W_b, \quad W_b < 1 \text{ GHz} \tag{3}$$

where k_1 and k_2 are environment-specific parameters. For NLOS with horizontal polarization, $k_1 = 5.75$ and $k_2 = 1.80$.

Table 7 presents the fade margin determined by Eq. (3) for various channel bandwidths considered in this paper. For a chosen target bandwidth, say B_t (in MHz), $F_\sigma(0.2) - F_\sigma(B_t)$ indicates the amount of enhancement in path loss due to the increased channel bandwidth.

Finally, considering 100 mW transmit power, the estimated SNR at B_t (MHz) is derived as

$$\begin{aligned} SNR(B_t)[\text{dB}] \;=\; & 10\log_{10} 0.1 - PL[\text{dB}] - N(B_t)[\text{dB}] \\ & + \big(F_\sigma(0.2) - F_\sigma(B_t)\big)[\text{dB}] \end{aligned} \tag{4}$$

where PL [dB] is the path loss measured at 200 kHz bandwidth, and $N(B_t)$ [dB] is the noise power at the bandwidth of B_t (MHz) which is given as [21]

$$N(B_t)[\text{dB}] = 10\log_{10}\big(k_B T(B_t \times 10^6)\big)$$

where $k_B = 1.38 \times 10^{-23}(J/K)$ is the Boltzmann's constant and $T = 290$ (K) is the room temperature.

B. Comparison of Estimated Downlink Capacity

The downlink capacity of Wi-Fi and Super Wi-Fi, denoted by C_w and C_s, respectively, are estimated by the Shannon capacity, such that

$$C_w \;=\; m_w B_w \cdot \log_2\big(1 + SNR_w(m_w B_w)\big), \tag{5}$$

$$C_s \;=\; m_s B_s \cdot \log_2\big(1 + SNR_s(m_s B_s)\big) \tag{6}$$

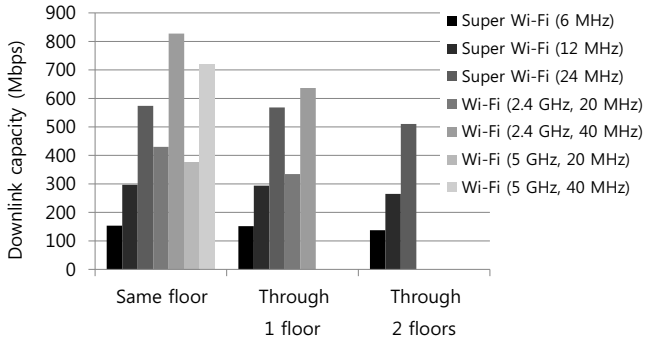

Fig. 9. Downlink capacity in the multi-floored scenario.

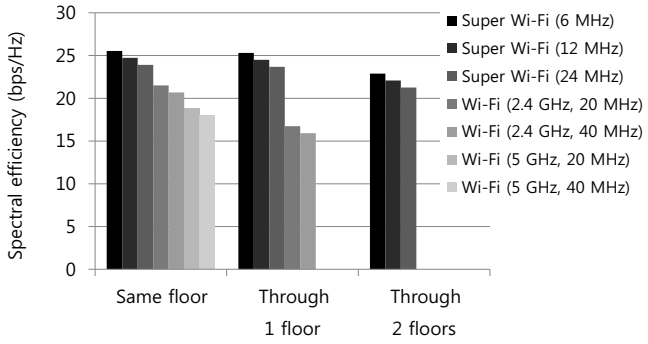

Fig. 10. Spectral efficiency in the multi-floored scenario.

where $B_w = 20$ MHz and $B_s = 6$ MHz are the channel bandwidths, SNR_w and SNR_s are the estimated SNR at the target bandwidth (i.e., $m_w B_w$ and $m_s B_s$) derived in scalar by Eq. (4), and $m_w \in \{1, 2\}$ and $m_s \in \{1, 2, 4\}$ are the channel bonding factors, i.e., the number of channels bonded together. By utilizing the FAF measured in subsection IV-B, the downlink capacity can be estimated not only for the single-floor case (i.e., the transceiver pair is located on the same floor) but also for the following two scenarios: (1) '± 1 floor' where the receiver is located one floor above or below the transmitter and (2) '± 2 floors' where the receiver is located two floors above or below the transmitter. In this case, the SNR in Eq. (4) is decreased by the number of floors multiplied by the FAF.[3]

Figs. 9 and 10 present the estimated downlink capacity and the spectral efficiency of Wi-Fi and Super Wi-Fi. In the 'same floor' case, 12 MHz Super Wi-Fi achieves 68.9% and 78.9% of 20 MHz Wi-Fi's capacity at 2.4 and 5 GHz, respectively, only using 60% of Wi-Fi's bandwidth. In addition, 24 MHz Super Wi-Fi achieves 133.3% and 152.6% of 20 MHz Wi-Fi's capacity at 2.4 and 5 GHz, respectively, using 20% larger bandwidth. In terms of spectral efficiency, however, Super Wi-Fi always performs better than Wi-Fi regardless of the channel bonding factors. Therefore, Super Wi-Fi is more efficient in utilizing the spectrum than Wi-Fi. In the '± 1 floor' case, 24 MHz Super Wi-Fi achieves 169.7% of 20 MHz Wi-Fi's capacity at 2.4 GHz and 89.2% of 40 MHz Wi-Fi's capacity at 2.4 GHz. That is, Super Wi-Fi can perform comparable to Wi-Fi only using 60% of Wi-Fi's bandwidth. In terms of spectrum efficiency, Super Wi-Fi becomes even more dominant than Wi-Fi. In the '± 2 floors' case, Super Wi-Fi with four bonded-channels can perform even much better than the Wi-Fi in the 'same floor' case, implying that a Super Wi-Fi network with channel bonding can support up to 5 floors with the downlink capacity as good as a Wi-Fi network covering a single floor.

Between the same floor and the '± 1 floor' cases, Super Wi-Fi presents only up to 0.97% degradation in capacity thus achieving almost-equal downlink rates across the three adjacent floors, whereas Wi-Fi presents up to 23.07% degradation.

Fig. 11 illustrates the estimated SNR map of Super Wi-Fi and Wi-Fi for each target bandwidth, revealing the following features. First, the SNR of Wi-Fi decreases fast with the distance, thus achieving much smaller coverage than Super Wi-Fi. Second, Super Wi-Fi supports stable and almost-evenly-distributed downlink capacity within its coverage. Finally, the shaded areas of Wi-Fi are much mitigated by Super Wi-Fi.

VI. CONCLUSION

In this paper, we have measured the characteristics of Wi-Fi and Super Wi-Fi in the same indoor environments in terms of WAF, FAF and path loss, from which their downlink capacities were estimated. Through the extensive measurement study, we have verified that Super Wi-Fi has superior characteristics indoors such as stronger wall-penetration and smaller path loss and thus it can provide wider coverage and more evenly-distributed data rates within its coverage compared to today's Wi-Fi. These results have revealed that Super Wi-Fi has great potential to become a successful application not only outdoors but also indoors, and Wi-Fi and Super Wi-Fi may be able to coexist in the same indoor structure complementing each other to provide enhanced wireless experience.

[3]For Wi-Fi at 5 GHz, we consider the same floor case only due to the absence of FAF measurement.

REFERENCES

[1] FCC, "Second memorandum opinion and order," *ET Docket No. 10-174*, Sept. 2010.
[2] Ofcom, "Regulatory requirements for white space devices in the UHF TV band," July 2012.
[3] ETSI, "EN 301 598 white space devices (WSD); wireless access systems operating in the 470 MHz to 790 MHz frequency band," Oct. 2012.
[4] H. Kim, K. Shin, and C. Joo, "Downlink capacity of super Wi-Fi coexisting with conventional Wi-Fi," in *Proc. IEEE GLOBECOM*, 2013.
[5] IEEE Std 802.11af-2013, "Part 11: Wireless LAN medium access control (MAC) and physical layer (PHY) specifications; amendment 5: TV white spaces operation," Feb. 2014.
[6] S. Seidel and T. Rappaport, "914 MHz path loss prediction models for indoor wireless communications in multifloored buildings," *IEEE Trans. Antennas Propag.*, vol. 40, no. 2, pp. 207–217, 1992.
[7] J.-F. Lafortune and M. Lecours, "Measurement and modeling of propagation losses in a building at 900 MHz," *IEEE Trans. Veh. Technol.*, vol. 39, no. 2, pp. 101–108, 1990.
[8] D. Porrat and D. Cox, "UHF propagation in indoor hallways," *IEEE Trans. Wireless Commun.*, vol. 3, no. 4, pp. 1188–1198, 2004.
[9] W. Honcharenko, H. Bertoni, J. Dailing, J. Qian, and H. Yee, "Mechanisms governing UHF propagation on single floors in modern office buildings," *IEEE Trans. Veh. Technol.*, vol. 41, no. 4, pp. 496–504, 1992.
[10] H. Cao, Z. Zhao, W. Ni, M. El-Hadidy, and T. Kaiser, "Measurement and ray-tracing of wideband indoor channel in UHF TV white space," in *Proc. ACM CogART*, 2011.
[11] C. Anderson and T. Rappaport, "In-building wideband partition loss measurements at 2.5 and 60 GHz," *IEEE Trans. Wireless Commun.*, vol. 3, no. 3, pp. 922–928, 2004.
[12] M. Lott and I. Forkel, "A multi-wall-and-floor model for indoor radio propagation," in *Proc. IEEE VTC-Spring*, 2001.

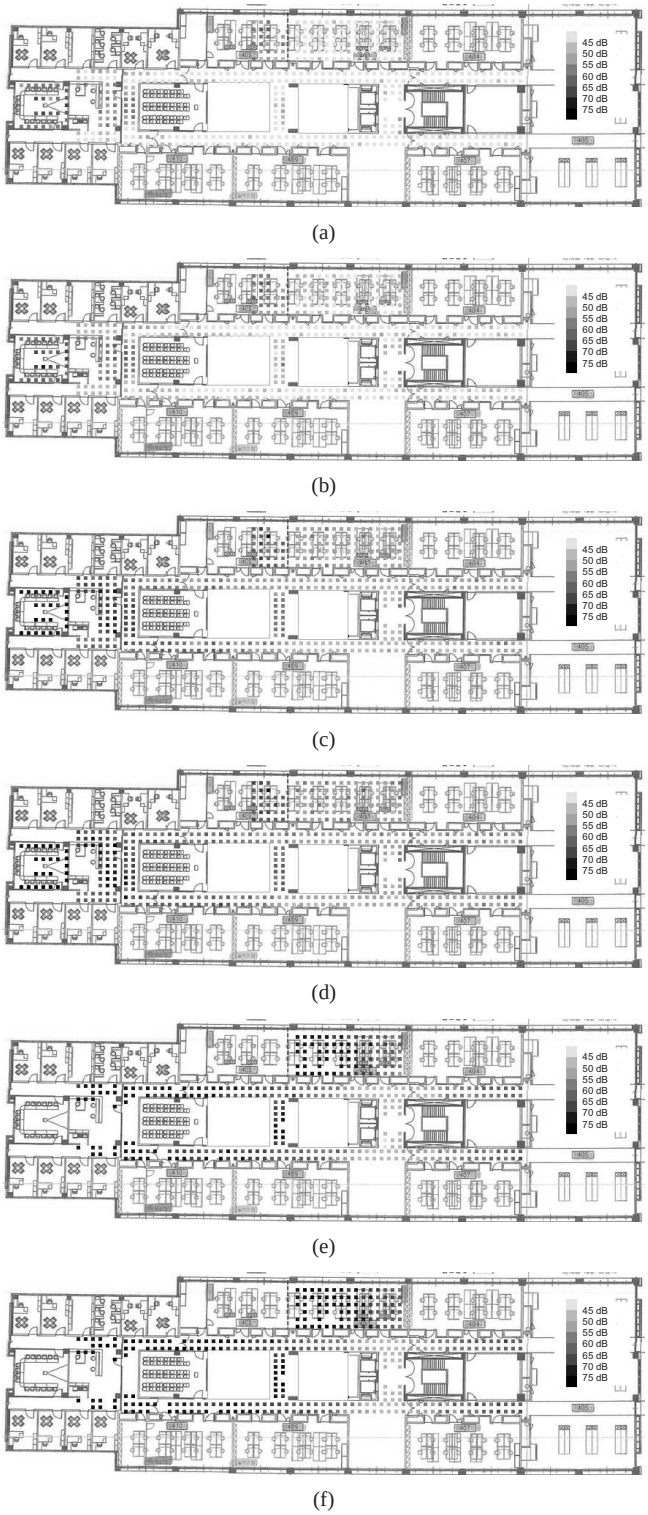

Fig. 11. SNR prediction in the single-floor scenario: (a) Super Wi-Fi (12 MHz bandwidth), (b) Super Wi-Fi (24 MHz bandwidth), (c) Wi-Fi (2.401 GHz, 20 MHz bandwidth), (d) Wi-Fi (2.401 GHz, 40 MHz bandwidth), (e) Wi-Fi (5.540 GHz, 20 MHz bandwidth), and (f) Wi-Fi (5.540 GHz, 40 MHz bandwidth).

[13] N. Sarkar and K. Sowerby, "Wi-Fi performance measurements in the crowded office environment: A case study," in *Proc. ICCT*, 2006.
[14] V.-H. Pham and J.-Y. Chouinard, "A Study on the channel and signal cross correlation of UHF DTV channels," in *Proc. ISSSE*, 2007.
[15] L. Simic, M. Petrova, and P. Mahonen, "Wi-Fi, but not on steroids: Performance analysis of a Wi-Fi like network operating in TVWS under realistic conditions," in *Proc. IEEE ICC*, 2012.
[16] Ettus Research, *Universal Software Radio Peripheral*. [Online]. Available: http://www.ettus.com
[17] *GNU Radio*. [Online]. Available: http://www.gnuradio.org/redmine/projects/gnuradio/wiki
[18] *RawOFDM*. [Online]. Available: http://people.csail.mit.edu/szym/ rawofdm/
[19] W. Stutzman and G. Thiele, *Antenna Theory and Design*. Hoboken, NJ: John Wiley & Sons, Inc., 2013.
[20] W. Malik, B. Allen, and D. Edwards, "Bandwidth-dependent modelling of smallscale fade depth in wireless channels," *IET Microw. Antennas Propag.*, vol. 2, no. 6, pp. 519–528, 2008.
[21] T. Rappaport, *Wireless communications: Principles and practice*. Upper Saddle River, NJ: Prentice Hall, 2002.

Gyumin Hwang is an assistant research engineer at Sysmate, Daejeon, Korea since 2014. He received his B.S degree in Computer Science and Engineering from Chungnam National University, Daejeon, Korea in 2012, and M.S degree in Electrical Engineering from the Ulsan National Institute of Science and Technology (UNIST), Ulsan, Korea in 2014. His research interests focus on high-speed packet processing systems and Super Wi-Fi in indoor environments.

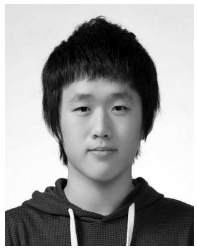

Kyubo Shin is a Ph.D. student at the School of Electrical and Computer Engineering, the Ulsan National Institute of Science and Technology (UNIST), Ulsan, Korea, since March 2015. He received his B.S. and M.S. degrees in Electrical and Computer Engineering from the UNIST, in 2013 and 2015, respectively. His research interest includes cognitive radio, Super Wi-Fi, and next-generation WLANs.

Sanghyeok Park was an undergraduate student at the School of Electrical and Computer Engineering, the Ulsan National Institute of Science and Technology (UNIST), Ulsan, Korea, while the research was performed, and received his B.S. degree in Electrical and Computer Engineering from the UNIST, in 2016. His research interest lies in wireless networking including Super Wi-Fi and LTE QoS.

Hyoil Kim (M'10-SM'16) is an Associate Professor at the School of Electrical and Computer Engineering, the Ulsan National Institute of Science and Technology (UNIST), Ulsan, Korea. Before joining the UNIST in 2011, he was a Postdoctoral Researcher in the IBM T.J. Watson Research Center, Hawthorne, NY, USA in 2010–2011. He received his B.S. degree in Electrical Engineering from Seoul National University, Seoul, Korea in 1999, and M.S. and Ph.D. degrees in Electrical Engineering: Systems from the University of Michigan in 2005 and 2010, respectively. His research interests lie in wireless networking with an emphasis on cognitive radios (CR), mobile cloud, next-generation WLAN and cellular networks, and 5G communications. He served as a TPC Member of various international conferences including IEEE INFOCOM (2014, 2016), ACM WiNTECH 2013, IEEE GLOBECOM (2011–2015), IEEE WCNC 2016, and IEEE PIMRC 2015, and also served as a Publicity Co-chair of ACM WiNTECH 2013.